The Journal of Experimental Biology 208, 141-155
Published by The Company of Biologists 2005
doi:10.1242/jeb.01358

Dendritic spike back propagation in the electrosensory lobe of *Gnathonemus petersii*

Leonel Gómez[1,2,*], Morten Kanneworff[2,3], Ruben Budelli[4] and Kirsty Grant[2]

[1]*Laboratory of Neuroscience, University of the Republic, Montevideo, Uruguay*, [2]*Unité de Neurosciences Intégratives et Computationnelles, CNRS, 91198 Gif-sur-Yvette, France*, [3]*Center for Sound Communication, Institute of Biology, University of Southern Denmark, DK-5230 Odense M, Denmark* and [4]*Department of Biomathematics, University of the Republic, Montevideo, Uruguay*

*Author for correspondence at address 1 (e-mail: leonel@biomat.fcien.edu.uy)

Accepted 26 October 2004

Summary

Spike timing-dependent plasticity that follows anti-Hebbian rules has been demonstrated at synapses between parallel fibers and inhibitory interneurons known as medium ganglionic layer (MG) neurons in the cerebellum-like electrosensory lobe of mormyrid fish. This plasticity is expressed when presynaptic activation is associated with a characteristically broad, postsynaptic action potential, lasting 7–15 ms, occurring within a window of up to 60–80 ms following synaptic activation. Since the site of plastic change is presumably in the apical dendrites, it is important to know where, when and how this broad spike is generated and the manner in which such events propagate within the intrinsic network of the electrosensory lobe.

The electrosensory lobe has a strict layered organization that makes the preparation suitable for one dimension current source density analysis. Using this technique in an '*in vitro*' interface slice preparation, we found that following either parallel fiber stimulation or an orthogonal field stimulus, a sink appeared in the ganglionic layer and propagated into the molecular layer. Intracellular records from MG somata showed these stimuli evoked broad action potentials whose timing corresponds to this sink. TTX application in the deep fiber layer blocked the synaptically evoked ganglionic layer field potential and the 'N_3' wave of the outer molecular layer field potential simultaneously, while the molecular layer 'N_1' and 'N_2' waves corresponding to synaptic activation of the apical dendrites remained intact. These results confirm the hypothesis that the broad spikes of MG cells originate in the soma and propagate through the molecular layer in the apical dendritic tree, and suggest the possibility that this backpropagation may contribute to 'boosting' of the synaptic response in distal apical dendrites in certain circumstances.

Key words: current source density, electric fish, backpropagating dendritic spike, electrosensory lobe, cerebellum-like network, *Gnathonemus petersii*.

Introduction

The notion of non-homogeneous neurons with interacting spatially diverse active responses challenges the classical view of orthodromic information flow, but this concept has become widely accepted during the last decade (Yuste and Tank, 1996). However, the integration of responses within multiple dendritic and somatic compartments, with different specific membrane properties, suggests complex computational mechanisms that are still poorly understood. This becomes still more complex when each neuron is considered as a dynamic unit, interacting with others in specific network arrangements.

The electrosensory lobe (ELL) of mormyrid electric fish is a cerebellar-like, layered structure with a very regular cytoarchitectural organization (Grant et al., 1996b; Meek, 1994; Meek et al., 1996), in which it is possible to study such complex integration in a meaningful functional context, and to clarify the computational roles of dendritic, somatic and axonal compartments. In this structure, incoming electrosensory activity is integrated with descending information driven by the electric organ corollary discharge (EOCD; Bell, 1981, 1982, 1989; Zipser and Bennett, 1976). Electroreceptor primary afferent (PA) terminal arborizations are mapped topographically in the granular cell layer of ELL. Corollary discharge information related to the electromotor command enters through three separate pathways that also integrate central feedback of past electrosensory history, proprioceptive information and probably other descending signals. Of these three pathways, we will consider here only that entering through parallel fibers arising from granule cells of the overlying cerebellar Eminentia Granularis posterior (EGp),

whose axons are distributed through the molecular layer of ELL. Parallel fibers synapse with the apical dendrites of several distinct populations of neurons whose cell bodies are situated in the ganglionic, plexiform and granular cell layers of ELL. These include Purkinje-like γ-amino butyric acid (GABA)-ergic interneurons (medium ganglionic layer cells: MG) and efferent projection neurons (large ganglionic layer neurons, LG; large fusiform neurons, LF).

MG neurons account for about 70% of the ELL ganglionic layer neuron population (Meek et al., 1996). These cells are easily recognized electrophysiologically by their characteristically broad action potentials (5–10 ms *in vitro*; up to 15 ms *in vivo*). Broad action potentials can be evoked *in vivo* by either corollary discharge input or electrosensory input, and *in vitro* by parallel fiber stimulation. Repetitive generation of broad spikes, for instance as might happen when the fish uses high speed electromotor scanning of the environment, has been associated *in vivo* with spike timing-dependent depression of synaptic responses to corollary discharge input (Bell et al., 1993). *In vitro*, associative pairing of parallel fiber EPSPs with post-synaptic broad action potentials has revealed a spike timing-dependent, anti-Hebbian plasticity rule: when the post-synaptic broad spike occurred within a window up to 60–80 ms following the presynaptic activation, the response to parallel fiber became depressed, whereas when a postsynaptic spike was evoked at other delays the synaptic response was frequently potentiated (Bell et al., 1997c, 1999; Grant et al., 1996a; Han et al., 2000a).

Given the extreme sensitivity of these plastic changes to the relative timing of presynaptic activation and postsynaptic broad spike generation (Bell et al., 1997c), it is important to know how and where broad spikes originate, how they propagate within the cell and what might be the consequences in terms of dendritic integration. Since MG cells are inhibitory interneurons, plasticity at parallel fiber synapses probably plays a central role in the temporal 'gating' of sensory reafference, and in the adaptive properties of corollary discharge driven, active filtering and sensory-motor coordination.

Previous work (Grant et al., 1998) has suggested the possibility that the broad spikes characteristic of MG neurons propagate back into the apical dendrites in the molecular layer. Rather similar broad action potentials have been described in Purkinje neuron dendrites of the cerebellum (Llinas and Nicholson, 1971) and there is a growing body of more recent *in vitro* evidence that the dendritic membrane can have electro-responsive properties, and actively supports propagation of action potentials in dendritic compartments in several other types of neurons (Regehr et al., 1992, 1993; Stuart and Sakmann, 1994; Spruston et al., 1995; Buzsáki and Kandel, 1998; Larkum et al., 2001; Golding et al., 2002). Of particular related interest are studies of the electrosensory lobe of the gymnotiform fish *Apteronotus leptorhynchus*, where Turner et al. (1994) have demonstrated the presence of Na^+ channels in the apical dendrites of pyramidal projection neurons and have shown that oscillatory bursting behavior is controlled through conditional backpropagation of dendritic spikes (Turner et al., 2002; Noonan et al., 2003).

The laminar organization of the ELL is clearly visible in the *in vitro* slice and makes this a suitable preparation to study the generation and propagation of broad action potentials in MG neurons (Grant et al., 1998). Stimulation of parallel fibers mimics EGp input to ELL and permits us to infer some rules for the local synaptic activation and postsynaptic cell responses. The synaptic responses evoked by parallel fiber stimulation can be recorded intracellularly at the level of the soma but have not been recorded intracellularly at the level of the distal apical dendrites where parallel fiber synapses occur. However, extracellular field potentials can be recorded easily across the layers of ELL and provide an alternative method of study. The layered organization of the ELL and the geometry and orientation of the principal cell types constitute an open field arrangement and the synchronous activation produced by their inputs, whether natural (driven by reafferent sensory input and the EOCD), or artificial (in response to electrical stimulation of the parallel fibers or the deep fiber layer), allow us to apply one-dimensional current source density (CSD) analysis to field potential recordings. The macroscopic pattern of current sinks and sources obtained with this method, produced by synchronous activity of local cell populations, together with anatomical data and intracellular recordings, are interpreted here to give insight into neuron behavior in response to specific input activation.

Materials and methods

Recordings were made in an *in vitro* slice preparation of the ELL of mormyrid fish of the species *Gnathonemus petersii* Günther 1862. A total of 12 fish were used for these experiments, ranging in length from 9 to 14 cm. Fish were housed in aquaria respecting their natural habitat, in a licensed animal housing facility conforming to French and international standards. Experimental procedures were carried out in accordance with international guidelines as set out by the European Convention for the Protection of Animals used for Experimental and other Scientific Purposes, the US Public Health Service Policy on Humane Care and use of Laboratory Animals (PHS Policy), and the National Institutes of Health Guide for the Care and use of Laboratory Animals (NIH Guide).

Slice preparation

Fish were deeply anesthetized by immersion in a cold aerated solution of tricaine methane sulfonate (MS 222 Sandoz, Schönenwerd, Switzerland) at a concentration of 100 mg l^{-1}. The skull was opened, and the brain was irrigated with ice-cold artificial cerebrospinal fluid (ACSF; for composition, see below). The valvula was retracted laterally, a vertical cut was made in the transverse plane immediately rostral to the ELL, the spinal cord was sectioned immediately caudal to the ELL, and the caudal brainstem block containing the ELL was removed. The brainstem block was transferred to

ice-cold ACSF for 60 s to harden it a little, and then the rostral cut surface was glued to a vibrating microtome block (Leica VT1000M, Nußloch, Germany) with cyanoacrylate glue, with the dorsal surface of the ELL facing the blade. The brain block was lightly supported by a coating of 16% gelatin dissolved in ACSF. 300–400 µm thick slices were cut in the transverse plane under ice-cold ACSF, using a sapphire blade (Delaware Diamond Knives, Wilmington, DE, USA). Slices were retrieved with a wide bore Pasteur pipette and transferred to a holding bath where they were kept submerged at room temperature, supported on small squares of Kodak lens paper that served to minimize direct handling. The ACSF used up to this point was almost Na-free, with sucrose replacing NaCl to reduce excitotoxic shock caused by the slicing (Aghajanian and Rasmussen, 1989). The composition of this low sodium ACSF was as follows (in mmol l^{-1}): NaCl 0, KCl 2.0, KH_2PO_4 1.25, $NaHCO_3$ 24, $CaCl_2$ 2.6, $MgSO_4.7H_20$ 1.6, glucose 20, and sucrose 213. The slices were transferred to an interface-recording chamber and superfused for 30 min with an ACSF solution containing a 1:1 mixture of low sodium ACSF and 'normal' ACSF (see below), before changing to 100% normal ACSF. The composition of the normal ACSF was as follows (in mmol l^{-1}): NaCl 124, KCl 2.0, KH_2PO_4 1.25, $NaHCO_3$ 24, $CaCl_2$ 2.6, $MgSO_4.7H_20$ 1.6, and glucose 20 (osmolarity: 290 mOsm. Both Na-free and normal ACSF were bubbled with 95% O_2 and 5% CO_2, bringing the pH to 7.2–7.4. The slices were supported in the recording chamber on several thickness of Kodak lens tissue and superfused with normal ACSF at room temperature (22–25°C), at a rate of 1–3 ml min^{-1} by gravity flow.

Stimulation

Parallel fibers were stimulated using monopolar tungsten electrodes (AM Systems, Sequim, WA, USA) whose tips had been lightly scraped on a sharpening stone to reduce tip resistance and then plated with gold to reduce electrode polarization. Stimulating current was delivered between a single such electrode in the tissue (negative pole) and a second similar electrode or silver wire (positive pole) in the bath outside the slice close to the external margin of EGp. The molecular, ganglionic, plexiform and superficial granule cell layers of ELL can be readily distinguished in the living slice under the operating microscope, allowing for accurate placing of stimulating and recording electrodes in these layers. Stimulating electrodes were placed in the outer half of the molecular layer, where parallel fibers run orthogonal to the apical dendrites of ganglionic layer neurons (Fig. 1). Stimuli were constant current pulses with a duration of 0.1 ms and amplitudes of 5–60 µA.

A second type of stimulation was used to activate ganglionic layer neurons directly, by generating an electric field across the layers of ELL, between a pair of platinum electrodes oriented in the axis of the apical dendritic trees and orthogonal to the parallel fiber beam (see Chan et al., 1988). One electrode was

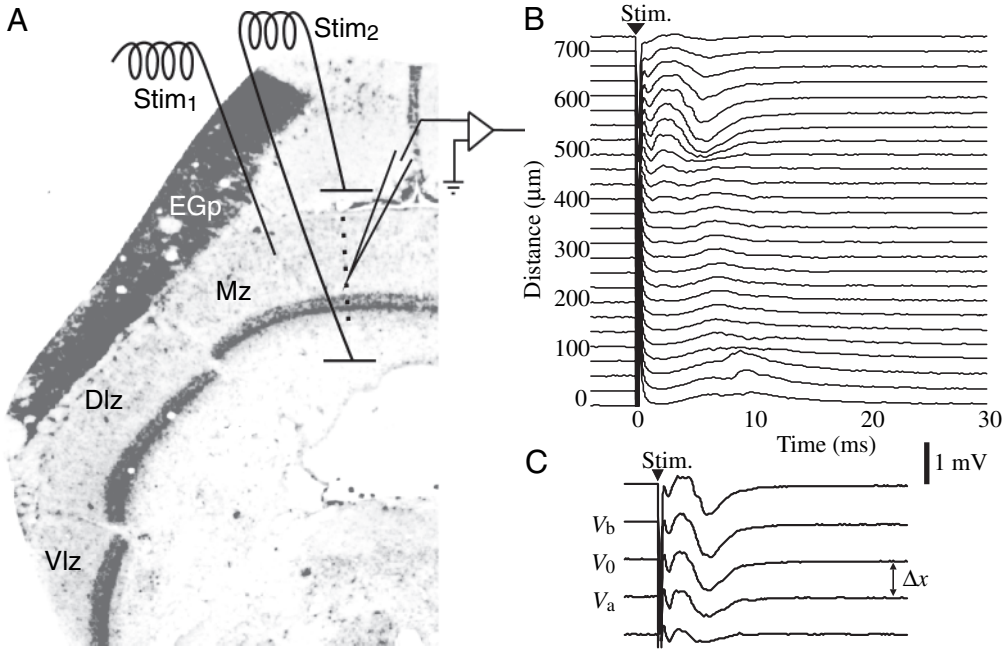

Fig. 1. Experimental setup and methods. (A) A semi-schematic representation of the ELL slice. $Stim_1$ represents the molecular layer stimulus and $Stim_2$ the trans-ELL field stimulation. The dotted line represents the alignment of successive recording sites. EGp, Eminentia Granularis posterior; Mz, dorsal zone, Dlz, dorsolateral zone and Vlz, ventrolateral zone of ELL. (B) Series of field potential recordings in response to molecular layer stimulation ($Stim_1$), made at successive sites through the layers of ELL as indicated by the dotted line in A, starting from the deep granular cell layer (distance 0 mm) to the outer molecular layer (distance 750 mm). See also Fig. 2 for an explanation of cell layers. (C) Enlargement of selected traces (V_b, V_0, V_a) from B, to illustrate how current source densities (CSD) are calculated. See Equation 3 in text.

placed external to the dorsal margin of the slice and the second was placed in the ventricle at the inner margin of ELL. A brief (1 ms) pulse of current was applied between these electrodes, generating an electric field across the layers. When the external electrode was made positive, current entered through the distal apical dendrites, producing hyperpolarization at this level, and left through the basal dendrites and probably the soma, producing a depolarization. This arrangement is illustrated in Fig. 1, which shows a diagram of the transverse ELL slice, indicating the positions of recording and stimulating electrodes ($Stim_2$).

Recording

The different zones and layers of ELL can be distinguished in the slice with the aid of a dissecting microscope. Most recordings were made in the medial zone of ELL because of its large size, but some were from the dorsolateral zone.

Intracellular recordings

Intracellular recordings were made with sharp glass micropipettes filled with 2 mol l^{-1} potassium methyl sulfate containing 2% biocytin (Molecular Probes, Eugene, OR, USA; Sigma, St Louis, MO, USA). Tip resistances were 150–200 MΩ. Based on previous studies, MG layer neurons could be distinguished by electrophysiological criteria alone, by the distinctive large, broad action potential that is present only in this cell type (Bell et al., 1997b; and see below).

Recorded neurons were labeled by intracellular iontophoresis of biocytin using DC current (tip positive or negative) of 0.2–0.5 nA for at least 5 min. Slices were fixed for 1 h in 2% paraformaldehyde and 2% glutaraldehyde in 0.1 mol l^{-1} phosphate buffer, pH 7, and labeled neurons were later revealed using the standard ABC process (Vector Laboratories, Burlingame, CA, USA).

Field potential recordings

Field potential recordings were made using pipettes filled with 3.0 mol l^{-1} NaCl having resistances of 3–6 MΩ. Recordings were made serially along a line perpendicular to the orientation of the layers of ELL, from the outer molecular layer to the intermediate layer, in conditions as constant as possible, as illustrated in Fig. 1A. An example of a series of recordings obtained at different levels through the molecular layer in response to parallel fiber stimulation is shown in Fig. 1B. Recording sites were separated by steps of 15, 25, 30 or 50 μm (Δx in Equation 3 below) depending on the brain size and, in some experiments, to check if the resolution of current source density analysis (see below) improved with smaller steps. On some occasions, different step sizes were tried in the same slice and it was found that decreasing the spatial step between recording points to less than 25–30 μm did not improve the resolution of the method. At each site, the recording electrode was placed at a depth of 40 μm from the surface of the slice. Responses were tested with an inter-stimulus interval of 2 s and 20–30 responses were averaged for each recording point in order to minimize the influence of response variability and improve the signal-to-noise ratio. Before calculating current source density, a digital low-pass filter was applied to further reduce noise (Richardson et al., 1987).

Current source density analysis (CSD)

When the tissue has no particular geometry, the current source density (S) at time t for a given point of a rectangular coordinate system is calculated as:

$$S(t,x,y,z) = -\left[\sigma_x\left(\frac{\partial^2 V(t)}{\partial x^2}\right)+\sigma_y\left(\frac{\partial^2 V(t)}{\partial y^2}\right)+\sigma_z\left(\frac{\partial^2 V(t)}{\partial z^2}\right)\right], \quad (1)$$

where σ_x, σ_y and σ_z are the conductivity tensors for the three x, y, z spatial dimensions respectively, and $V(t)$ is the extracellular voltage. However, the ELL complies with what is called an 'open field' geometrical arrangement (Hubbard et al., 1969; Johnston and Miao-Sin Wu, 1995): it is a layered structure with the principal axis of majority of cells oriented perpendicular to the plane of the layers. If this array of neurons is activated by a synchronous synaptic input (i.e. parallel fiber stimulation) a dipole is established between the apical dendrites and the somas. Currents that run in the directions parallel to the layers cancel out, and the problem is reduced to one spatial dimension, as is shown in Equation 2 (Haberly and Shepherd, 1973; Mitzdorf, 1985; Richardson et al., 1987):

$$S(t,z) = -\sigma_z\left(\frac{\delta^2 V(t)}{\delta z^2}\right). \quad (2)$$

The empirical process of calculation of the CSD from field potential (FP) recordings is given in Equation 3:

$$\frac{\partial^2 V(t)}{\partial x^2} \cong \left(\frac{V_b - 2V_o + V_a}{\Delta x^2}\right) \propto i(t). \quad (3)$$

The waveforms defined by the symbols V_a, V_o and V_b are shown in Fig. 1C.

CSDs are represented as color maps to facilitate visualization of the continuity of processes in time and space. In each color map (see for example Fig. 2) green represents zero; colors from green to red indicate sinks (inward currents), and colors from green to blue represent sources (outward currents).

Since CSD was calculated in one dimension and the value of the extracellular conductivity was not determined, CSD waveforms cannot be considered absolute quantitative estimates of current density. Units are therefore not provided on CSD profiles. Rather, CSD estimates are used to compare the qualitative characteristics of sink-source relationships in ELL slices. Based on similar reasoning, in order to make some patterns more evident, we applied an arc-tangent function to the CSD data. This function has a sigmoid shape, having asymptotes $-\pi/2$ and $\pi/2$ when the variable tends to $-\infty$ and $+\infty$, respectively, and is equal to 0 when the variable is 0. This procedure amplifies low amplitude events while those of large amplitude saturate. This operation is symmetrical with respect to 0.

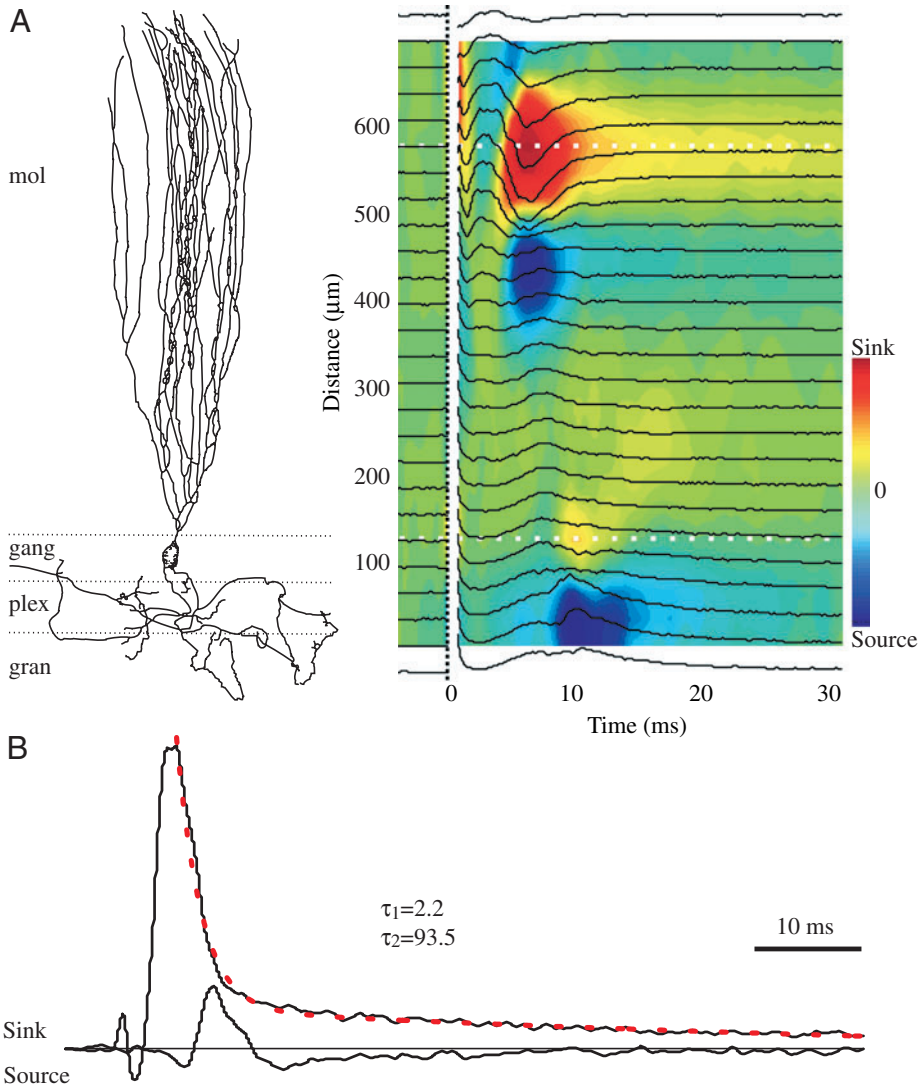

Fig. 2. Response obtained with a low intensity molecular layer stimulation. (A) Left: reconstruction of a medium ganglionic (MG) layer cell showing its extension through the layers of ELL, as a reference for the events shown in the right panel. mol, molecular layer; gang, ganglionic layer; plex, plexiform layer; gran, granular layer. Right: one-dimensional current-source density (CSD) pseudocolor map with field potential recordings superimposed. Green to red are sinks and green to blue are sources as is shown with the color bar on the right. (B) Plot of current density evolution with time, for the two locations marked by white dotted lines in the CSD pseudocolor map in A: at 550 mm (upper line) in the molecular layer, and at 110 mm (bottom line) in the ganglionic layer. A second order exponential function (red dotted line) was fitted to the molecular layer CSD profile decay and the corresponding time constants τ_1 and τ_2 are shown above the graph.

Pharmacology

In order to produce a selective block of sodium-dependent spikes in neuron somata in the ganglionic layer, in some experiments, a drop of tetrodotoxin (TTX; 0.5–1.0 mmol l^{-1}) was applied by pressure injection into the surface of the slice from a glass micropipette. The micropipette was positioned about 25 µm below the slice surface in the deep fiber layer. The TTX took several minutes to diffuse from the injection site, reaching the ganglionic layer before the molecular layer.

Data analysis

Data were recorded using an Axoclamp 2B amplifier (Axon Instruments, Union City, CA, USA) and stored on the hard disk of a computer *via* a Labmaster interface (Scientific Solutions, North Chelmsford, MA, USA) and Acquis1 software written by Gerard Sadoc (C.N.R.S., Gif sur Yvette, France). Quantitative measurements were made using Acquis1 or Matlab (MathWorks, Natick, MA, USA) software and plotted using Matlab.

Results

The first section below describes field potential responses to electrical stimulation of the molecular layer of ELL slices (a more complete description can be found in Grant et al., 1998) and introduces CSD analysis calculated from these field potentials. Different stimulation types and patterns were used: single, paired and multiple pulse protocols are analyzed. Responses to electric field stimulation applied perpendicularly to the layers of ELL are considered in detail. Finally, responses evoked using each of the two types of stimuli (molecular layer stimuli and field stimuli) are compared.

In the second section of the Results, intracellular recordings of responses to molecular layer stimulation are presented in order to compare synaptic and single cell spiking events with the population events revealed by CSD analysis. Finally, pharmacological tools were used to investigate the identities of phenomena described.

Field potentials and CSD analysis

CSD calculated from sequentially recorded field potentials

make it possible to observe processes that are time-locked to a triggering event (in this case the parallel fiber stimulus), provided that the field potentials remain relatively constant over the process of sequential recording of the whole series. Field potentials were large enough to be observed throughout the different layers of ELL and were recorded at successive points passing through the layers, in the same plane as the apical dendritic arborization of ganglionic layer neurons. The shape of field potentials evoked in ELL was not affected by the averaging process and low-pass filtering. We first describe the typical CSD patterns obtained with parallel fiber stimulation (single and paired stimulation pulses), and then responses evoked by trans-ELL field stimulation. The effects of multiple stimulation protocols are described for both types of stimulation and differences and similarities are discussed.

Molecular layer stimulation

Fig. 2 shows the CSD pattern obtained in response to low intensity molecular layer stimulation, plotted as a color map. Field potential recordings are superimposed on the CSD color map. The CSD abscissa shows time in ms and the ordinate represents distance from the starting recording point in the granular layer of ELL. An MG neuron is drawn to the same scale to facilitate location of events observed in the CSD and field potential plots in relation to the cell compartments. The stimulation artifact has been removed. Red areas are current sinks, i.e. current flowing into the cell. Blue areas are current sources: i.e. current flowing out of the cell. Green, as is shown in the color bar, represents the zero value, when no current flows either in or out of the cells.

The earliest event following the stimulation artifact in the field potential records is a small negative wave (N_1) with a delay shorter than 1 ms. Wave N_1 occurs 'on beam' to the stimulation site between 400 mm and 800 mm in the figure. Grant et al. (1998) suggested that this wave corresponds to the parallel fiber action potential. Parallel fibers are oriented in the same transverse plane as the layers of ELL so their activation does not fit the open field condition and, consequently, this activity can not be analyzed reliably with the one dimensional CSD technique. However, since N_1 amplitude is maximum in front of the stimulation electrode and decays to both sides (up and down in Fig. 2A), a positive concavity (i.e. the yellow-orange spot coinciding with N_1 in Fig. 2A) will appear when the second derivative is calculated. This may also be produced in part by activity in the presynaptic terminal (Mitzdorf, 1985).

Beginning at around 3 ms, also on the same beam, a second negative wave (N_2) can be observed; this reaches a minimum at approximately 6 ms. Grant et al. (1998) postulated that this wave is generated by the EPSP produced by the parallel fibers in apical dendrites of ELL cells. In the CSD plot, a sink can be seen at the same delay, also peaking around 6 ms. The red spot is flanked by two blue spots that correspond to the current sources generated by the central sink. This sink with its companion sources represents the most intense and longest activity observed.

The time course of this process is illustrated in Fig. 2B. The rise time of the current sink peak was 2 ms and this then decayed as a second order exponential function. Time constants for decay of the response (red dotted line in Fig. 2B) were: τ_1=2.2 ms and τ_2=93.5 ms. This profile is very similar to that of the parallel fiber EPSP observed with somatic intracellular recordings (see fig. 11a in Grant et al., 1998).

The spatial distribution of the sources is tightly related to the length constant of the activated cells (Mitzdorf, 1985). The manner in which current spreads away from the point of synaptic activation is governed by the electrotonic properties of the cells, and from this it is possible to estimate the mean length constant of apical dendrites. The term length constant is generally used to describe a passive steady-state response property, and may not be entirely applicable to the present context since small active events may be occurring locally in the dendrites, linked to synaptic activation, that are below the resolution of field potential recordings. However, we may derive some information about what is going on at the population level from spatial plots of CSD and even though active conductances are involved, this 'length constant' is a measure of how far a depolarization propagates. Fig. 3A shows the CSD corresponding to the timing and spatial distribution of N_2 in a gray-scale color map. Fig. 3B shows the spatial profile of current densities at a given time *t* after the stimulus (shown by the dotted black line in Fig. 3A), corresponding to the peak of synaptic activation. The 'length constant' of the active cells can be estimated from the spatial decay of the sources from their peak amplitude. In the inset of Fig. 3, an exponential function was fit to the distal tail of the current profile across the layers, giving a length constant of 34.24±7.06 mm. In different slices this value varied but was never larger than 90 μm (mean 60 μm, S.D.=23, *N*=7). Since in every case an exponential function fits the experimental results, it can be assumed that in this slice preparation, the process is mainly passive. The range of estimated length constants is rather short compared with values calculated for neurons in some mammalian structures and suggests non-compact cells that would allow mainly spatially restricted interactions within the dendritic arborization. This may be important for the integrative properties and the consequences of synaptic plasticity in ELL neurons.

Around 9 ms after the beginning of the parallel fiber stimulation artifact, another sink appears at the level of the proximal apical dendrites in the ganglionic layer (Fig. 2A). This sink peaks in the range 7–10 ms and lasts 4–10 ms. It is preceded and followed by a source. This tri-phasic negative/positive/negative sequence can be better appreciated in Fig. 2B, which shows the evolution of current density with time, in the molecular layer and in the ganglionic layer. This pattern is typically produced by an active process. First, excitatory inputs in the apical dendrites spread passively producing a source in the ganglionic layer. The resulting excitation of the ganglionic layer then generates a sink at this level and finally, excitation propagates back into the molecular layer (see also Fig. 4), generating a new source in the ganglionic layer. Note that the simultaneous source associated

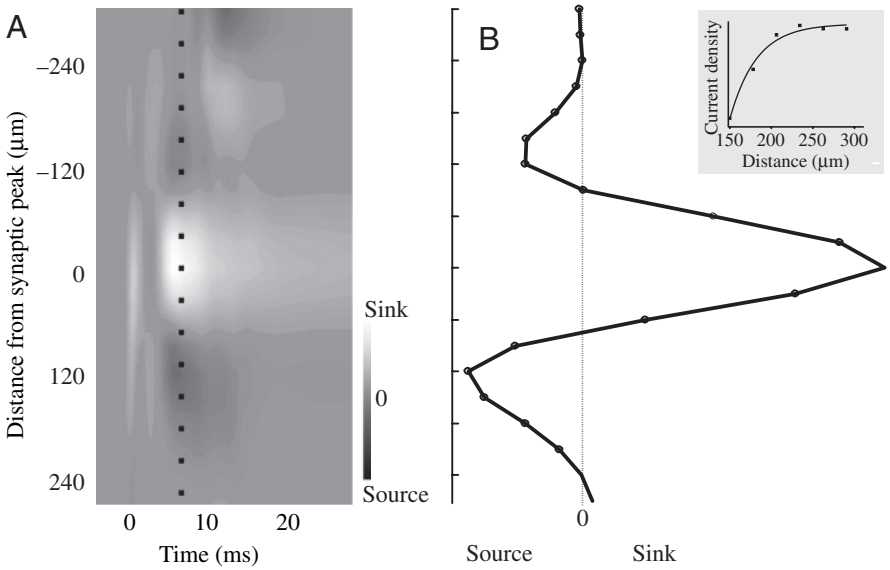

Fig. 3. Method for estimating 'length constant' of apical dendrites. (A) CSD in a gray-scale map for data obtained with molecular layer stimulation. A typical Source/Sink/Source spatial pattern can be observed (distal towards top). (B) Spatial distribution of current density profile at time indicated by dotted line in A, corresponding to the peak of the synaptic sink (distal towards top). Inset in B shows the exponential function fitted to the distal tail of the synaptic source.

with the ganglionic layer sink is located asymmetrically, appearing principally in the plexiform and granular layers (see lower blue spot in Fig. 2A, centered at 10 ms and 20 mm). This means that the current tends to leave cells through their basal dendrites, although it is possible that some current produced by the molecular layer, parallel fiber-evoked synaptic sink may also contribute to this source in the deeper layers.

Paired pulse stimulation in the molecular layer

Paired pulse facilitation (ppf) of the field potentials evoked by ELL molecular layer stimulation is commonly observed. This involves both the parallel fiber EPSP-related component of the field potential (N_2) and also a third negative wave that has been called N_3 (Fig. 4A; Grant et al., 1998). The N_3 wave is not always present; its amplitude and morphology are rather variable and, in some cases there are more complicated patterns of response, including additional waves. In this subsection we investigate field potential responses to paired pulses applying CSD analysis.

In Fig. 4A a CSD color plot is shown with the corresponding field potential recordings superimposed, in response to paired pulse stimulation of the molecular layer with an inter-stimulus delay of 50 ms. An MG cell outline is presented on the left, to aid relating events to cell compartments. The response evoked by the first stimulus was similar to those described previously but is different in two ways, probably due to a more intense stimulation of the parallel fibers. The first of these differences is that the sink originating in the ganglionic layer is very well defined in this preparation and extends, with increasing latency, outward through the proximal molecular layer. This suggests an active process that propagates in the direction of the molecular layer from its starting point in the ganglionic layer. This excitation coincides in delay and duration with the broad spikes seen in intracellular recordings in response to parallel fiber stimulation, and shows that in certain circumstances, it is possible to obtain a synchronized population response originating in the region of the soma layer, that backpropagates into the apical dendritic arborization following a single stimulus. The second noticeable difference is the presence of a second positive peak (sink) that appears in the molecular layer sink, approximately 10 ms later than the initial parallel fiber-evoked peak and at the same distance from the soma. This second peak has a lower amplitude than the first (yellow in the color scale axis while the preceding peak is dark red). and coincides with the N_3 wave of the field potentials (arrow in Fig. 4A).

In response to the second stimulation pulse both field potential negative peaks, N_2 and N_3, are larger, and N_3 can now be traced down as far as the ganglionic layer. The latency of N_3 decreases gradually as the recording site approaches the ganglionic layer. In the underlying CSD color map, a sink clearly follows the N_3 wave through the layers, repeating the pattern of latency change. This suggests an active process propagating from the ganglionic layer towards the distal region of the apical dendrites, that spreads with a velocity of approximately 0.05–0.07 m s^{-1}. The reduction in sink amplitude in the intermediate part of its trajectory (between 300–500 mm on the ordinate) could be due to the superposition with the source of the population excitatory postsynaptic potential (EPSP).

In order to better appreciate the characteristics of this process we subtracted the response evoked by the first parallel fiber stimulus from the response evoked by the second one (Fig. 4B). This operation highlights the components that are increased (or decreased) by the double stimulus. Sinks that are facilitated appear in red. This showed that the initial synaptic response to the second parallel fiber stimulus was potentiated (probably the result of presynaptic potentiation; Grant et al., 1998). Backpropagation of the sink initiated at the ganglionic layer also became more visible using paired pulse parallel fiber stimulation protocols.

In Fig. 4B, this sink can be followed clearly (white dotted

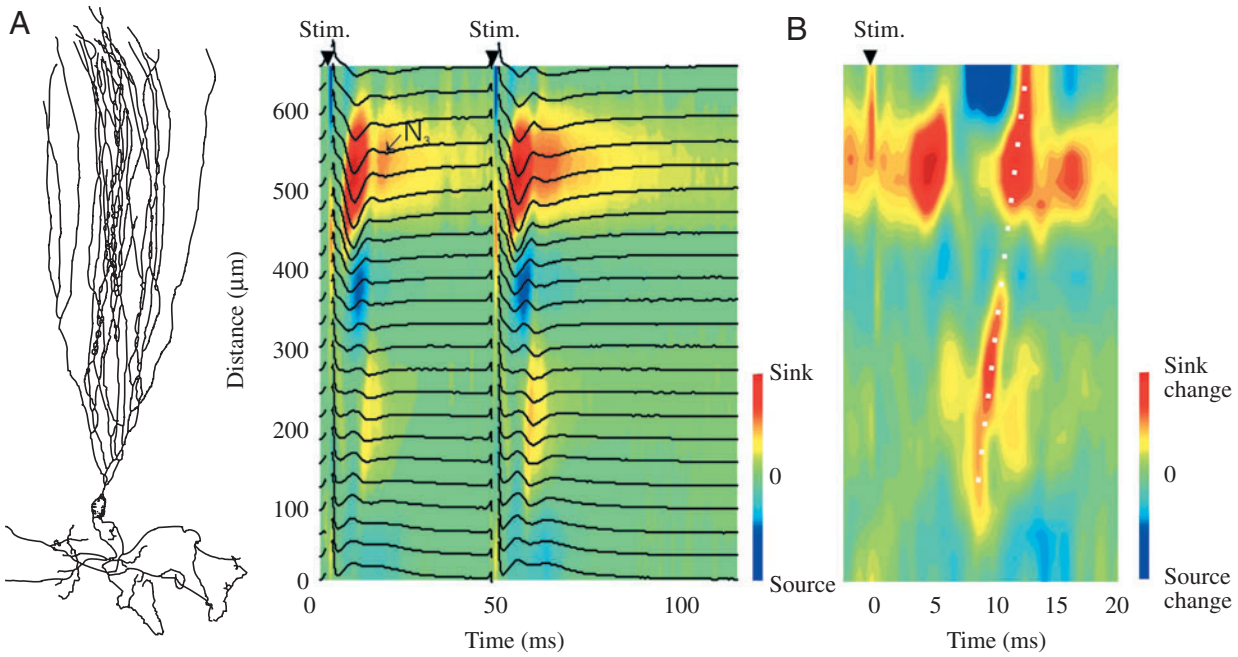

Fig. 4. Responses to paired pulse molecular layer stimulation. (A) Left: MG cell reconstruction to serve as a spatial reference. Right: CSD pseudocolor map with field potential traces superimposed. Arrowheads above traces indicate the times of stimulus application (Stim). (B) Calculation of the difference between the first and second responses. Color bar on the right indicates observed increase or decrease in entering current density when the first response was subtracted from the second. Dotted line indicates the spatial displacement and time course of the backpropagated event. Note that both the initial sink (associated with field potential N_2) and the later sink (associated with field potential N_3) are increased in response to the second stimulus pulse.

line) until it reaches the level of the molecular layer synaptic sink. While the backpropagating sink was reduced where it crossed the synaptic source, it was markedly increased when it joined the synaptic sink. Although this effect was not quantified, the apparent increase of the back propagated event seems to be greater than expected from linear summation with the potentiated EPSP, suggesting a boosting of the backpropagated dendritic spike by the EPSP, similar to that described, for example, in hippocampus (Migliore et al., 1999; Watanabe et al., 2002).

Trans-ELL field stimulation, single pulses

When a brief (1 ms) electric field stimulus applied across the layers of ELL was used to activate the network (see Materials and methods and Fig. 1A: $Stim_2$), we observed a different pattern of response, illustrated in Fig. 5. Using this stimulation, Fig. 5B shows inversion of the stimulus current peak (black dotted line and arrows) somewhere between the ganglionic and granular layers; thus, current enters the cells all along the apical dendritic tree (hyperpolarizing at this level) and leaves the cells (producing depolarization) close to the ventral pole, at the level of the axon initial segment and the basal dendrites. This stimulus pattern is a consequence of the intrinsic organization of the ELL and is a reflection of the distribution of membrane resistance of the neurons whose dendrites compose the highly oriented network.

Field potential recordings are superimposed over the color map representing the calculated CSD. Field potential traces corresponding to the granular and plexiform layers, situated at the level of the soma and basal dendrites of the MG cell profile on the left, presented a sharp negative wave that lasted about 5 ms, followed by a positive wave of smaller amplitude that lasted more than 10 ms. This pattern gradually inverted as the recording site moved outwards through the ganglionic and molecular layers. Molecular layer field potentials were composed of an initial large positive wave, immediately after the stimulation artifact, followed by a smaller negative wave whose latency increased linearly with increasing distance towards the outer molecular layer. Both positive and negative field potentials lasted about 5 ms. In the CSD color map representation it can be seen that a well-defined sink coincides with the field potential negative wave. Nevertheless, the sink duration is shorter than the negative wave (2–3 ms), reflecting the more precise time resolution of this technique. The sink increases in amplitude from the deep granular layer to the ganglionic layer, where it reaches a maximum, and then decreases again in the molecular layer.

Fig. 5B shows the time function of the CSD at three different levels (indicated by white dotted lines in Fig. 5A), to better appreciate its changing shape. Another interesting point is that this sink produced by trans-ELL field stimulation originates more deeply than the sink evoked by molecular layer stimulation. In the case of field stimulation illustrated in Fig. 5A, the corresponding sources can be observed on both

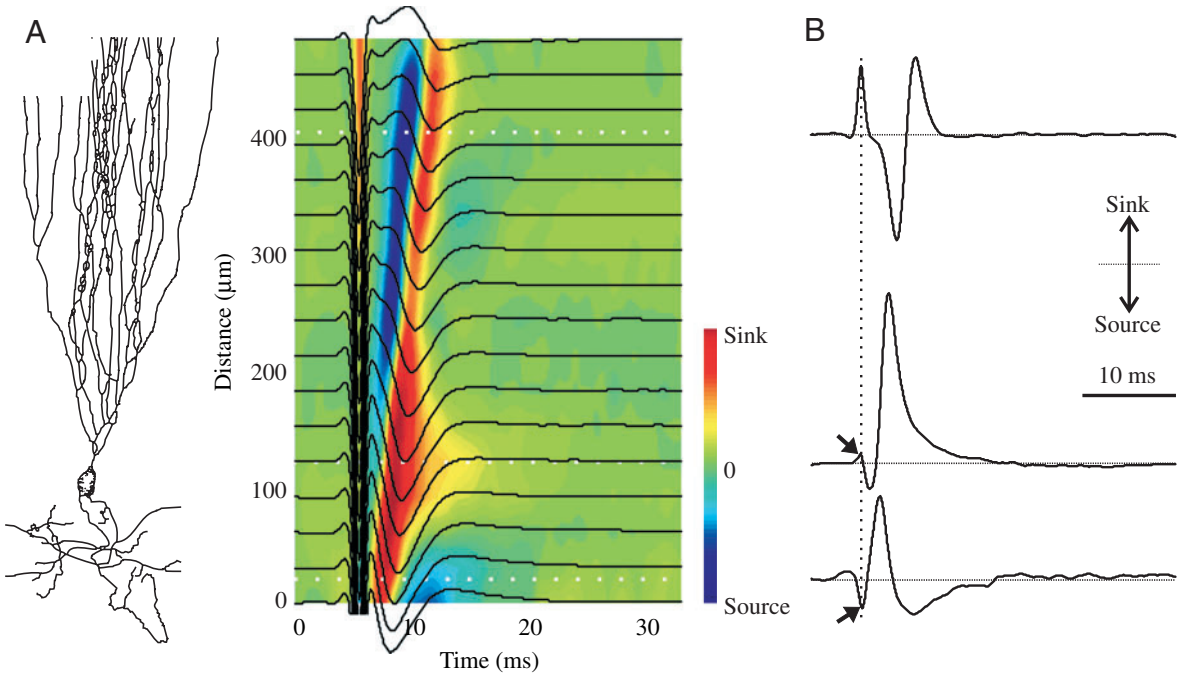

Fig. 5. Responses to trans-ELL field stimulation. (A) Left: cell profile as a spatial reference. Right: CSD as a pseudocolor map with field potential recordings superimposed. (B) Selected CSD traces from A aligned with the corresponding height in the pseudocolor map in A. These show that the stimulus current peak (black dotted line) inverts (see arrows) somewhere between the ganglionic and granular layers; thus, current enters the cells all along the apical dendritic tree and leaves the cells close to the ventral pole, at the level of the axon initial segment and the basal dendrites.

sides of the sink. The source that is generated distal to the active zone is well defined and continuous, but the proximal source is divided in two by the prolongation of the sink at the ganglionic layer and is mainly concentrated in the plexiform and granular layers. The propagation velocity of the sink out into the molecular layer was calculated as 0.09 m s^{-1} from this data.

Multiple molecular layer and field stimulation

To compare the responses obtained with each type of stimulus in similar conditions, molecular layer and field stimuli were applied alternately, in the same slice. The experiment was done with a multiple pulse protocol to observe whether or not there was potentiation in the two cases. The top panel of Fig. 6A shows the CSD of the response to a sequence of three molecular layer stimuli; the bottom panel shows the CSD of the responses to a sequence of three field stimuli. In both cases the basic CSD patterns are as described previously. In response to molecular layer stimulation (Fig. 6A, top) potentiation is very clear, even between the second and the third stimuli, exhibiting a build-up of the response to the train of stimuli. Potentiation is clear in both components of the response: the synaptic event and the back propagated event. In contrast, responses obtained with field stimulation showed no potentiation (Fig. 6A, bottom). On the contrary, successive stimuli produced progressively reduced responses. For the examples shown in Fig. 6, the calculated velocities of backpropagated processes were 0.07 m s^{-1} for the molecular layer stimulation-evoked event and 0.09 m s^{-1} for the field stimulation-evoked event.

In Fig. 6B a magnified view of the third response to molecular layer stimulation is shown to highlight some response features that were observed in approximately half of the experiments carried out (4 out of 9 experiments). (1) In some cases a sink appeared midway between the site of synaptic entry and the ganglionic layer response (arrow in Fig. 6B). This yellow spot could be an active response of the proximal dendrites produced by the EPSP. (2) The second variation with respect to the patterns described above was observed when the ganglionic sink was in fact composed of two distinct sinks occurring at the same depth, one a little earlier than the other (arrowheads in Fig. 6B). Both had a tendency to propagate back into the molecular layer, but it was always the case that when these two sinks appeared together, that the earlier one was thinner, more elongated, and seemed to propagate outward faster. There may be several explanations for this behavior. It is possible that the two sinks correspond to the spiking activity of different cell populations, e.g. synchronized LG cells and then MG cells. Alternatively, since MG cells are by far the most numerous and probably contribute most to CSD images, part of this population may fire an early spike and the remainder may first be inhibited by the stimulus and then fire on the delayed parallel fiber EPSP. Intracellular records show that MG neurons do not fire two broad action potentials in response to single parallel fiber stimulation.

Intracellular recordings

Responses to molecular layer stimulation were recorded intracellularly in different cell types. Our purpose was to establish a relationship between the population events illustrated in the field potential study above and the behavior of individual cells, and for this reason only recordings obtained from MG cells are presented here. MG neurons are by far the most numerous cell type in the ganglionic layer of ELL and their apical dendritic trees account for probably more than 80% of the dendritic component of the molecular layer. It is therefore likely that MG cell responses will weight the field potentials evoked by molecular layer stimulation proportionally more than those of other cell types contributing to the collective evoked responses.

Fig. 7 illustrates responses recorded in an MG cell. A single parallel fiber stimulus of weak intensity repeated at long intervals produced only a sub-threshold post-synaptic EPSP. But when the same stimulus was repeated at intervals in the range of those used by the fish in highly attentive electromotor scanning (50 ms), the probability of evoking first small narrow spikes, together with occasional medium sized spikes (Fig. 7, arrowhead), and then full sized broad spikes, quickly increased. Traces from top to bottom are examples of responses obtained applying increasing number of stimulation pulses to the parallel fibers. In addition to the typical MG cell spiking responses mentioned before, is interesting to note long-lasting depolarization that builds up in response to repeated stimuli separated by 50 ms intervals, and also the train of small spikes lasting several hundred milliseconds that is superimposed on this depolarization.

The inset in Fig. 7 shows a graph of the probability of evoking a broad spike plotted as a function of the number of stimuli applied; this reaches a value of 1 after four stimuli separated by 50 ms intervals. (In this example, probability started at zero because the intensity of the individual pulses was chosen so that a

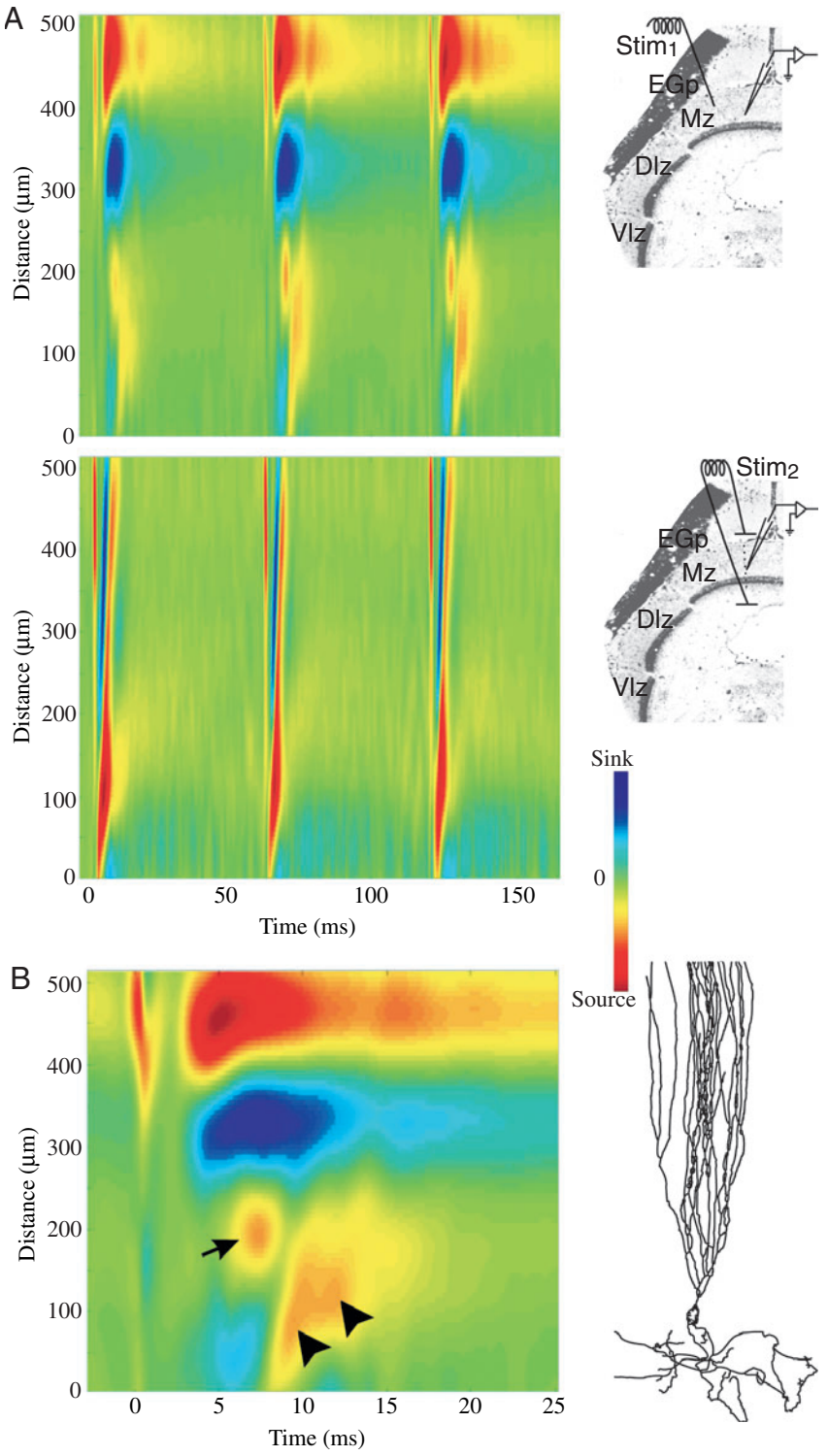

Fig. 6. Responses to multiple pulses, compared using the two stimulation methods (molecular layer and trans ELL field) described in the text. (A) (top) Three successive stimuli to the molecular layer produced increasing facilitation; (bottom) three successive trans-ELL field stimuli resulted in depression of 2nd and subsequent responses. Data were acquired concomitantly by applying the two different stimuli in alternate sweeps. (B) The third response in A (top) is shown with an expanded timebase. Arrow shows a sink that appeared midway between the site of synaptic entry and the ganglionic layer response, which was observed in some, but not all, cases. Arrowheads show that the ganglionic sink was in fact composed of two distinct sinks occurring at the same depth, one a little earlier than the other. Both sinks had a tendency to propagate back into the molecular layer. It was always the case that when these two sinks appeared together, the earlier one was thinner, more elongated, and seemed to propagate outward faster. Abbreviations, see legend to Fig. 1.

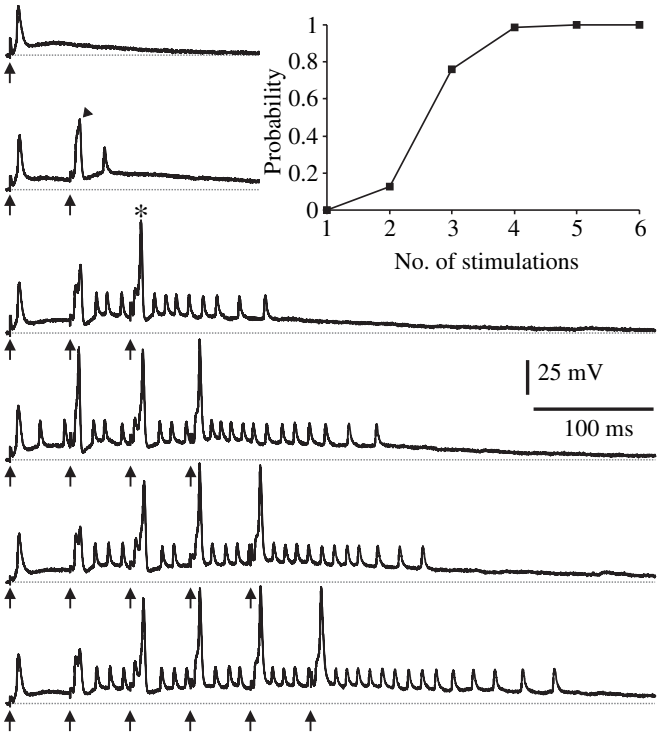

Fig. 7. Intracellular recordings from an MG cell. Molecular layer stimulation (arrows) was adjusted initially below threshold for evoking a postsynaptic action potential and was then applied repetitively at a frequency representative of the natural electric organ discharge (EOD) rhythm during increased sensory attention. Postsynaptic responses increased with the number of stimuli, leading to the generation of partial (arrowhead) and then full backpropagating broad spikes (asterisk), and to increasing numbers of small narrow spikes (probably axon spikes). Note that a slow depolarization, lasting several hundred ms, builds up with repetitive stimulation. The inset (top right) shows a plot of the probability of evoking a broad spike as a function of the number of stimuli applied.

single stimulus did not produce a broad spike. With higher stimulation intensities a single stimulus could evoke a broad spike.) Note that with three stimuli, the protocol used for extracellular recording experiments, the probability of obtaining a broad spike response was in the order of 0.75. Although the timing of broad spikes was somewhat variable, most reached their peak amplitude around 10 ms after the beginning of the stimulus artifact, which coincides precisely with the peak of the ganglionic layer sink described in previous section.

The pharmacological separation of synaptic events and active postsynaptic responses using TTX

To discriminate between the synaptic component of the response obtained with molecular layer stimulation and the second negative peak of the response, and to determine if the latter is truly an active process backpropagating from the ganglionic and plexiform layers, across the molecular layer of the ELL, an experiment was designed to separate the two components (Fig. 8). While recording simultaneously the evoked responses in the distal molecular layer and in the ganglionic layer, a micro-injection of the sodium channel blocker TTX was made just below the slice surface in the deep fiber layer. Since the diffusion of TTX within the slice is a transient process we could not use CSD analysis to study this phenomenon, and instead, interpretation of the results depends on the established relation between N_3 and the presumed backpropagated process. Field potentials recorded simultaneously in the molecular layer and the ganglionic layer are represented as color maps against time from TTX application, at the top right and bottom right of Fig. 8, respectively. Initially, the characteristic N_2 and N_3 wave patterns were observed in the molecular layer and correspond to the two horizontally running blue zones in the top panel (N_1 was masked by the stimulation artifact). The doubled peaked positive wave typical of the ganglionic layer is shown in the bottom panel of Fig. 8. In this representation, the abscissa represents time between successive sweep records and the ordinate shows time within a sweep. The stimulation artifact was masked and its place appears in white in the figure.

The TTX took a little more than 45 s to diffuse from the application point in the deep fiber layer to the recording point in the ganglionic layer. At this time the response disappeared completely in the plexiform and ganglionic layer level (Fig. 8, bottom). This was accompanied by the simultaneous disappearance of the N_3 wave in the distal molecular layer (the lower horizontal blue region seen in Fig. 8, top), although no changes were yet visible in the N_2 wave. Approximately 1.5 min later, when the TTX reached the distal molecular region, N_2 also disappeared. This experiment demonstrates the origin of the events that produce the N_3 wave at the distal molecular layer, showing that it is generated in the ganglionic-plexiform layers and depends on the activation of sodium channels.

Discussion

The one-dimensional CSD methodology used here combines the known anatomy and physiology of ELL and field potential measurements, and provides a better space–time resolution of the events in the cellular assemblies than field potential recording alone. Although this method only reveals events that involve populations of cells acting synchronously in regular laminated structures, these conditions are complied with naturally in this preparation, since all of the activity is synchronized with the stimulus (there are no cells with synchronized spontaneous activity in this preparation *in vitro*). A drawback of this technique when applied using averages of sequentially recorded field potentials is its inability to show patterns changing with time, such as plastic adaptation. However it is powerful in showing stimulus-locked events long enough to overlap in time. These conditions are in general fulfilled by EPSPs evoked by a synchronous synaptic input but in this particular preparation the same conditions are also met

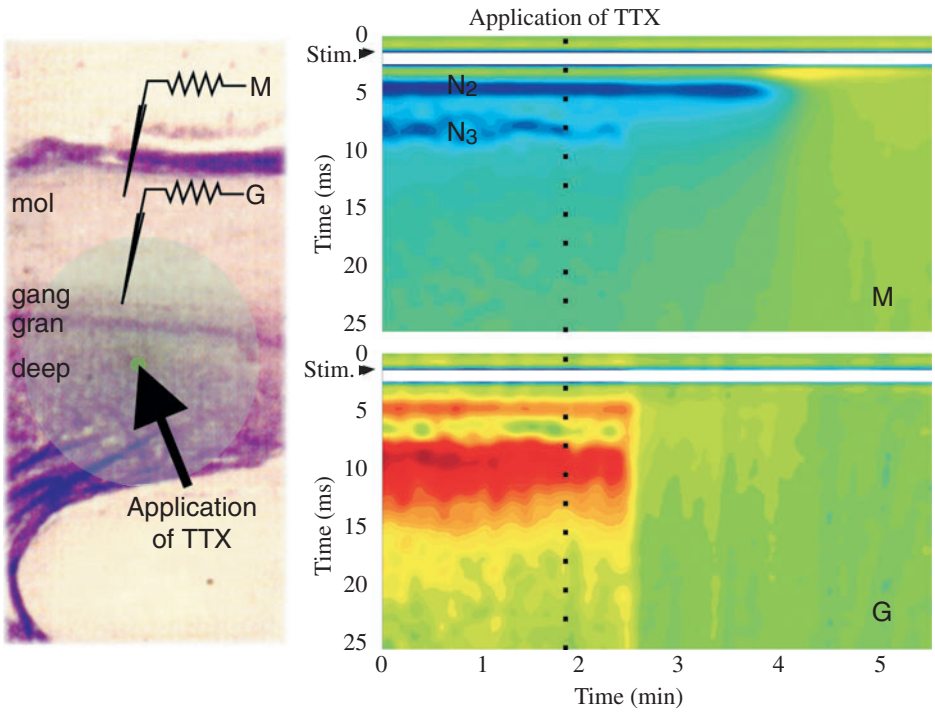

Fig. 8. Blocking of backpropagation by TTX. (Left) Diagram of experimental setup showing position of recording electrodes in outer molecular layer (M) and ganglionic layer (G). Green spot and shaded area represent site of TTX application in the deep fiber layer and its diffusion outwards. (Right) Color representation of field potentials obtained from M (top) and G (bottom) recording points. N_2 and N_3 are indicated in the upper panel. Dotted line indicates the moment at which TTX was applied. The ganglionic layer response disappeared 45 s after TTX application and simultaneously N_3 disappeared in the molecular layer response. N_2 persisted for a further 1.5 min.

by the long duration (5–15 ms) broad spikes characteristic of MG cells.

In response to molecular layer stimulation, the first large event that appears in CSD plots is clearly related to the N_2 wave of the field potential, and most probably corresponds to the EPSP produced by the molecular layer stimulation of the parallel fibers, which has both (AMPA)- and *N*-methyl-D-aspartate (NMDA)-receptor mediated components. However, several studies using rather similar stimulation paradigms in slices of the hippocampus and the neocortex, have suggested that it is also possible that such stimulation may evoke local active processes initiated in the dendrites and that these components cannot always be discriminated in field potentials (Turner et al., 1984, 1991; Stuart and Hausser, 2001). While CSD analysis cannot discriminate spiking and synaptic events either, this technique gives an average of the principal events most likely to occur, their spatial distribution and temporal progression through the network. From this we can say that although it is possible that responses to synchronous molecular layer stimulation may also include local dendritic spikes, these probably do not propagate towards the soma because in this case a downward propagating sink should appear. Although the relationship between N_2 and parallel fiber synaptic activation was already suggested from previous electrophysiological studies (Grant et al., 1998), the CSD analysis applied here shows the time course of this process more clearly and reproduces that of EPSPs recorded intracellularly quite precisely, thus allowing a more accurate characterization of the global synaptic input following parallel fiber stimulation.

The synaptic sink is immediately flanked by its sources, meaning that the current leaves the cells in the immediate vicinity of the synaptic input. We found that the spatial decay of the 'tail' sources were well fit by an exponential function. This indicates that spatial decay of current after synaptic activation is mainly passive. An estimate of a population 'length constant' can be made as a measure of these passive properties. From the present results, very short values were estimated for these 'length constants', compared with the usual values obtained in other preparations. For hippocampal pyramidal cells, for example (Turner, 1984), expressing the length of dendrites in units of space constants gives estimated values between 0.32 and 0.91, whereas our estimations for ELL MG cell apical dendrites are 4–6 space constants. This suggests that the cells may have the possibility of generating local domains for synaptic interactions with parallel fibers, decoupled from other synapses nearby. Pushing this reasoning further, this could allow specific plastic modulation of the weights of individual, or restricted groups of parallel fiber synapses.

The negative wave N_3 visible in field potential recordings can be traced up from the ganglionic to the molecular layer. From comparison of field potential data with the timing of events measured intra- and extracellularly, a relationship was postulated between the N_3 wave and intracellular broad spikes (Grant et al., 1998). However, as stated before, relationships between field potentials and cellular events are uncertain and further proof was required to be sure of this interpretation.

The regular narrow spikes fired by most neurons are difficult to see with CSD analysis since, being brief, they require extreme synchronization in order for their sum to produce visible current sources and sinks. However, the MG cells, which constitute at least 70% of the ganglionic layer soma population and probably give rise to a still larger proportion of the apical dendrites contained in the molecular layer, fire

consistently broad action potentials. Because of their long duration, the sinks/sources in individual cells produced by broad spikes would tend to add together sufficiently to produce events visible by the CSD analysis method, even if their generation were not completely synchronous. Confirming this supposition, CSD analyses show that following synaptic activation, a second sink always appears in the ganglionic layer, peaking approximately 10 ms later than the beginning of the stimulation artifact. Broad spikes appear in intracellular recordings with approximately the same latency range. In many cases (depending of the stimulus strength and/or number of stimulating pulses), this sink travels from the ganglionic-plexiform region towards the apical dendrites. This CSD event is clearly related to the N_3 wave of the field potentials, although it is sometimes present in the absence of a well defined N_3 field potential. These results provide further support to the hypothesis of broad spike propagation into the apical dendritic tree. This is confirmed by the abolition of the N_3 wave concomitantly with the disappearance of activity at the ganglionic level when TTX is applied to the deep fiber layer of the slice.

An active process with similar characteristics can also be produced with field stimulation, showing that this phenomenon does not necessarily depend on parallel fiber synaptic activation in all circumstances. Although there is overall similarity, some differences exist between the synaptic-evoked and field-evoked processes. In particular, synaptic-evoked processes are more complex, sometimes showing decomposition into two distinct phenomena that could be due to differential synaptic activation of two cell populations. Another difference is seen in responses to repetitive stimulation. When the late backpropagating response is evoked by a train of parallel fiber stimuli, it builds up in a manner that parallels the increase in the molecular layer synaptic related event. The increase in synaptic efficacy leads to more effective triggering of the dendritic population spike and is probably the result of both presynaptic potentiation and prolonged postsynaptic depolarization.

In contrast, when a backpropagating event is evoked directly by a trans-ELL field stimulus, a decrease in the amplitude of successive responses to a train of stimuli was observed. This resembles paired pulse depression that has been described for the granular layer field potential response to stimulation in the intermediate layer. This depression is sensitive to bicuculline and has been interpreted as the result of lateral inhibition in the inner layers of the ELL (Han et al., 2000b), mediated by large GABA-ergic inhibitory interneurons (large myelinated interneurons: LMI; Meek et al., 2001). The dendrites of these inhibitory neurons do not extend into the molecular layer and these cells would not be activated by parallel fiber stimulation, thus explaining the different response behavior to repetitive stimulation at these different sites.

The backpropagation velocity of dendritic spikes through the molecular layer was relatively slow: approx. 0.05–0.09 m s^{-1} in ELL, compared with, for example, 0.67 m s^{-1} estimated for backpropagated spikes in rat cortex by Buszáki and Kandel (1998). The small but consistent differences in the velocity of the backpropagated events in ELL estimated from the two stimulation procedures used here, might be explained by the long-lasting sub-threshold depolarization that builds up postsynaptically during repetitive molecular layer stimulation (Fig. 7), possibly facilitating dendritic spike propagation. The short 'length constant' estimated from source decays can explain this, and at the same time suggests the need for an active process as a means of intracellular signaling to communicate between distant locations. Changes in the propagation velocity as were reported in *Apteronotus* (Turner et al., 1994; Lemon and Turner, 2000), underlying complex dynamics in the cell activation (conditional backpropagation, ghostbursting), have not been observed in this preparation although small changes could exist that are below the resolution level of the method used here.

Further indirect evidence that the propagated CSD event described here corresponds to the backpropagation of the broad action potential comes from the experiment where it was shown that the probability of evoking a broad spike increased monotonically with the number of parallel fiber stimulation pulses. Increasing the number of stimuli increased the probability of evoking a broad spike in individual cells, and the increase in global population activity will be reflected in the population spike seen in the CSD analysis.

The conduction of the signal from the synaptic location to the triggering point for this backpropagated phenomenon seems to be mainly passive, but on some occasions a spot of activation was seen as the synaptic potential was translated down through the molecular layer towards the soma in the ganglionic layer. It is possible that these 'hot spots' occur where apical dendrites converge at their proximal point of origin and that at the population level, they represent the initiation and propagation of dendritic spikes towards the soma. This is also a possible explanation for the medium-sized spikes that can be recorded in the soma (see arrowhead in second trace in Fig. 7). The typical geometry of MG cells shows 10–20 very spiny distal apical dendrites that arise from 3–6 short primary dendrites, which in turn arise from a small soma, 10–12 mm in diameter (Grant et al., 1996b; Meek et al., 1996). This could provide the necessary anatomical substrate for summation of signals spreading through distal apical dendrites towards the soma, reaching the threshold for broad spike generation somewhere near the soma: in the primary dendrites, in the soma itself, or at the axon hillock. The local initiation of dendritic regenerative events and their partial or full propagation towards the soma has been described in different types of neurons in a number of studies (e.g. Regehr et al., 1993; Schwindt and Crill, 1997; Stuart et al., 1997; Martina et al., 2000; Kloosterman et al., 2001).

Previous pharmacological studies (Sugawara et al., 1999) have shown that broad spikes are a Na^+-dependent phenomenon and that they resist removal of extracellular calcium. It is therefore supposed that voltage-dependent Na^+ channels exist in the dendrites and the possibility that there are dendritic action potential initiation sites cannot be ruled out.

This has also been suggested by Turner et al. (1994) who, using an antibody directed against sodium channels, have described punctate regions of immunolabel separated by nonlabeled expanses of membrane, over the entire extent of basal dendrites and also the apical dendritic tree, in the gymnotid electrosensory lobe.

Repetitive parallel fiber stimulation produced both increasing amplitude of the population EPSP and an increase in the population backpropagated event. Coincidence of these events may in fact result in amplification of the backpropagating dendritic response and boosting of synaptically evoked activity in distal dendrites, as suggested by the result illustrated in Fig. 4B. Thus the response properties of molecular layer dendrites could depend in a non-linear manner on the frequency and intensity of parallel fiber input, involving both pre- and post-synaptic mechanisms. A similar boosting of the backpropagated event has been described in hippocampus and related to enhanced excitability produced by the inactivation of A-type potassium channels. The consequent long-lasting depolarization has been shown to be important for the induction of long-term potentiation (LTP) (Magee and Johnston, 1997; Watanabe et al., 2002; Frick et al., 2004).

In ELL, paired pulse, or short interval repetitive stimulation at frequencies in the order of those used in the natural EOD rhythm of the fish, increased both the probability of full spike backpropagation and MG cell output (spikelets; Fig. 7) producing short term facilitation. This type of change in dendritic response properties may be expressed in certain well identified behavior patterns associated with increased sensory attention, e.g. high speed regular electric organ discharge (EOD) observed during active exploration, or the novelty response, in which there is a transient increase in EOD in response to a sudden change in the environment.

This appears to be different from the spike timing-dependent anti-Hebbian plasticity that has been demonstrated at parallel fiber synapses, whose expression also depends on the presence of postsynaptic broad spikes (Grant et al., 1996a; Bell et al., 1997c, 1999; Han et al., 2000a). In this case, repetitive association between synaptic activation and the postsynaptic generation of broad spikes leads to synaptic depression. It has been suggested that this plasticity plays a role in updating corollary discharge-driven feedback signals representing central predictions of the sensory world, documented *in vivo* (Bell et al., 1997a).

These different mechanisms for the modulation of dendritic integration in MG cells may play different functional roles. Since MG cells are inhibitory interneurons, most likely reciprocally interconnected as well as being pre-synaptic to output neurons, the resultant effects of their activity on output neurons will depend on a delicate balance of the interplay of inhibition and disinhibition. The transition from short-term facilitation to synaptic depression is not yet well understood and better knowledge of the mechanisms involved would have interesting computational implications for information processing in the basic microcircuit of the ELL, as well as in other cerebellum-like or cortical structures in which sensory processing depends greatly on descending feedback. To arrive at a full understanding of the mechanisms of adaptive filtering processes, these functional properties of MG interneurons would need to be considered in terms of the dynamics of local circuits responding to the dual activation of both sensory afferents and descending corollary discharge.

Conclusion

MG interneurons are by far the most abundant type of neurons in the ganglionic layer of ELL and it is at synapses between parallel fibers with these neurons that spike timing-dependent plasticity is most readily expressed. Because these neurons are inhibitory and provide a major source of input to the somatic region of efferent neurons, and possibly also reciprocally inhibit each other, it is likely that plastic modulation of their integrative properties will play a central role in signal processing in ELL. Backpropagated broad spikes could provide a mechanism to relate activity in compartments proximal to the soma (sensory inputs, deep path of the corollary discharge input, axonal spikes) with distal input arriving *via* parallel fibers. Linked to the mechanism of synaptic plasticity, dendritic backpropagation would thus provide a vector for the dynamically changing relationship between descending and sensory inputs.

List of abbreviations

ACSF	artificial cerebrospinal fluid
AMPA	α-amino-3-hydroxy-5-methyl-4-isoxazolepropionic acid
CSD	current source density
EGp	eminentia granularis posterior
ELL	electrosensory lobe
EOCD	electric organ corollary discharge
EPSP	excitatory postsynaptic potential
FP	field potential
GABA	γ-amino butyric acid
LF	large fusiform
LG	large ganglionic
LMI	large myelinated interneuron
LTP	long-term potentiation
MG	medium ganglionic
NMDA	*N*-methyl-D-aspartate
PA	electroreceptor primary afferent
ppf	paired pulse facilitation
TTX	tetrodotoxin

This work was partially supported by the European Commission (contracts CI1*-CT92-0085 and IST-2001-34712), an ECOS grant (U97B03) to K.G. and R.B., and a grant from the CSIC – Universidad de la República, Uruguay, to R.B and L.G.

References

Aghajanian, G. K. and Rasmussen, K. (1989). Intracellular studies in the facial nucleus illustrating a simple new method for obtaining viable motoneurons in adult rat brain slices. *Synapse* **3**, 331-338.

Bell, C. C. (1981). An efference copy which is modified by reafferent input. *Science* **214**, 450-453.

Bell, C. C. (1982). Properties of a modifiable efference copy in an electric fish. *J. Neurophysiol.* **47**, 1043-1056.

Bell, C. C. (1989). Sensory coding and corollary discharge effects in mormyrid electric fish. *J. Exp. Biol.* **146**, 229-253.

Bell, C., Bodznick, D., Montgomery, J. and Bastian, J. (1997a). The generation and subtraction of sensory expectations within cerebellum-like structures. *Brain. Behav. Evol.* **50**, 17-31.

Bell, C. C., Caputi, A. and Grant, K. (1997b). Physiology and plasticity of morphologically identified cells in the mormyrid electrosensory lobe. *J. Neurosci.* **17**, 6409-6423.

Bell, C. C., Caputi, A., Grant, K. and Serrier, J. (1993). Storage of a sensory pattern by anti-Hebbian synaptic plasticity in an electric fish. *Proc. Natl. Acad. Sci. USA* **90**, 4650-4654.

Bell, C. C., Han, V. Z., Sugawara, Y. and Grant, K. (1997c). Synaptic plasticity in a cerebellum-like structure depends on temporal order. *Nature* **387**, 278-281.

Bell, C. C., Han, V. Z., Sugawara, Y. and Grant, K. (1999). Synaptic plasticity in the mormyrid electrosensory lobe. *J. Exp. Biol.* **202**, 1339-1347.

Buzsáki, G. and Kandel, A. (1998). Somadendritic backpropagation of action potentials in cortical pyramidal cells of the awake rat. *J. Neurophysiol.* **79**, 1587-1591.

Chan, C. Y., Hounsgaard, J. and Nicholson, C. (1988). Effects of electric fields on transmembrane potential and excitability of turtle cerebellar Purkinje cells in vitro. *J. Physiol.* **402**, 751-771.

Frick, A., Magee, J. and Johnston, D. (2004). LTP is accompanied by an enhanced local excitability of pyramidal neuron dendrites. *Nat. Neurosci.* **7**, 126-135.

Golding, N. L., Staff, N. P. and Spruston, N. (2002). Dendritic spikes as a mechanism for cooperative long-term potentiation. *Nature* **418**, 326-331.

Grant, K., Bell, C. and Han, V. (1996a). Sensory expectations and anti-Hebbian synaptic plasticity in cerebellum- like structures. *J. Physiol. Paris* **90**, 233-237.

Grant, K., Meek, J., Sugawara, Y., Veron, M., Denizot, J. P., Hafmans, T. G., Serrier, J. and Szabo, T. (1996b). Projection neurons of the mormyrid electrosensory lateral line lobe: morphology, immunohistochemistry, and synaptology. *J. Comp. Neurol.* **375**, 18-42.

Grant, K., Sugawara, Y., Gomez, L., Han, V. Z. and Bell, C. C. (1998). The mormyrid electrosensory lobe in vitro: physiology and pharmacology of cells and circuits. *J. Neurosci.* **18**, 6009-6025.

Haberly, L. B. and Shepherd, G. M. (1973). Current density analysis of summed evoked potentials in *Opossum prepyriform* cortex. *J. Neurophysiol.* **36**, 789-802.

Han, V. Z., Grant, K. and Bell, C. C. (2000a). Reversible associative depression and non-associative potentiation at a parallel fiber synapse. *Neuron* **27**, 611-622.

Han, V. Z., Grant, K. and Bell, C. C. (2000b). Rapid activation of GABAergic interneurons and possible calcium independent GABA release in the mormyrid electrosensory lobe. *J. Neurophysiol.* **83**, 1592-1604.

Hubbard, J. I., Llinas, R. and Quastel, D. M. J. (1969). Electrophysiological analysis of synaptic transmission. London: Edward Arnold.

Johnston, D. and Miao-Sin Wu, S. (1995). *Foundations of Cellular Neurophysiology*. Cambridge, Massachusetts: MIT Press.

Kloosterman F., Peloquin P. and Leung L. S. (2001). Apical and basal orthodromic population spikes in hippocampal CA1 *in vivo* show different origins and patterns of propagation. *J. Neurophysiol.* **86**, 2435-2444.

Larkum, M. E., Zhu, J. J. and Sakmann, B. (2001). Dendritic mechanisms underlying the coupling of the dendritic with the axonal action potential initiation zone of adult rat layer 5 pyramidal neurons. *J. Physiol*. **533**, 447-466.

Lemon, N. and Turner, R. W. (2000). Conditional spike backpropagation generates burst discharge in a sensory neuron. *J. Neurophysiol.* **84**, 1519-1530.

Llinas, R. and Nicholson, C. (1971). Electrophysiological properties of dendrites and somata in alligator Purkinje cells. *J. Neurophysiol.* **34**, 532-551.

Magee, J. C. and Johnston, D. (1997). A synaptically controlled, associative signal for Hebbian plasticity in hippocampal neurons. *Science* **275**, 209-213.

Martina, M., Vida, I. and Jonas, P. (2000). Distal initiation and active propagation of action potentials in interneuron dendrites. *Science* **287**, 295-300.

Meek, J. (1994). Microcircuitry of the mormyrid electrosensory lateral line lobe. *Eur. J. Morphol.* **32**, 279-282.

Meek, J., Grant, K., Sugawara, Y., Hafmans, T. G., Veron, M. and Denizot, J. P. (1996). Interneurons of the ganglionic layer in the mormyrid electrosensory lateral line lobe: morphology, immunohistochemistry, and synaptology. *J. Comp. Neurol.* **375**, 43-65.

Meek, J., Hafmans, T. G., Han, V., Bell, C. C. and Grant, K. (2001). Myelinated dendrites in the mormyrid electrosensory lobe. *J. Comp. Neurol.* **431**, 255-275.

Migliore, M., Hoffman, D. A., Magee, J. C. and Johnston, D. (1999). Role of an A-type K^+ conductance in the back-propagation of action potentials in the dendrites of hippocampal pyramidal neurons. *J. Comput. Neurosci.* **7**, 5-15.

Mitzdorf, U. (1985). Current source-density method and application in cat cerebral cortex: investigation of evoked potentials and EEG phenomena. *Physiol. Rev.* **65**, 37-100.

Noonan, L., Doiron, B., Laing, C., Longtin, A. and Turner, R. W. (2003). A dynamic dendritic refractory period regulates burst discharge in the electrosensory lobe of weakly electric fish. *J. Neurosci.* **23**, 1524-1534.

Regehr, W., Kehoe, J. S., Ascher, P. and Armstrong, C. (1993). Synaptically triggered action potentials in dendrites. *Neuron* **11**, 145-151.

Regehr, W. G., Konnerth, A. and Armstrong, C. M. (1992). Sodium action potentials in the dendrites of cerebellar Purkinje cells. *Proc. Natl. Acad. Sci. USA* **89**, 5492-5496.

Richardson, T. L., Turner, R. W. and Miller, J. J. (1987). Action-potential discharge in hippocampal CA1 pyramidal neurons: current source-density analysis. *J. Neurophysiol.* **58**, 981-996.

Schwindt, P. C. and Crill, W. E. (1997). Local and propagated dendritic action potentials evoked by glutamate iontophoresis on rat neocortical pyramidal neurons. *J. Neurophysiol.* **77**, 2466-2483.

Spruston, N., Schiller, Y., Stuart, G. and Sakmann, B. (1995). Activity-dependent action potential invasion and calcium influx into hippocampal CA1 dendrites. *Science* **268**, 297-300.

Stuart, G. J. and Hausser, M. (2001). Dendritic coincidence detection of EPSPs and action potentials. *Nat. Neurosci.* **4**, 63-71.

Stuart, G. J. and Sakmann, B. (1994). Active propagation of somatic action potentials into neocortical pyramidal cell dendrites. *Nature* **367**, 69-72.

Stuart, G., Schiller, J. and Sakmann, B. (1997). Action potential initiation and propagation in rat neocortical pyramidal neurons. *J. Physiol.* **505**, 617-632.

Sugawara, Y., Grant, K., Han, V. and Bell, C. C. (1999). Physiology of electrosensory lateral line lobe neurons in *Gnathonemus petersii*. *J. Exp. Biol.* **202**, 1301-1309.

Turner, D. A. (1984). Segmental cable evaluation of somatic transients in hippocampal neurons (CA1, CA3, and dentate). *Biophys. J.* **46**, 73-84.

Turner, R. W., Lemon, N., Doiron, B., Rashid, A. J., Morales, E., Longtin, A., Maler, L. and Dunn, R. J. (2002). Oscillatory burst discharge generated through conditional backpropagation of dendritic spikes. *J. Physiol. Paris* **96**, 517-530.

Turner, R. W., Maler, L., Deerinck, T., Levinson, S. R. and Ellisman, M. H. (1994). TTX-sensitive dendritic sodium channels underlie oscillatory discharge in a vertebrate sensory neuron. *J. Neurosci.* **14**, 6453-6471.

Turner, R. W., Meyers, D. E., Richardson, T. L. and Barker, J. L. (1991). The site for initiation of action potential discharge over the somatodendritic axis of rat hippocampal CA1 pyramidal neurons. *J. Neurosci.* **11**, 2270-2280.

Turner, R. W., Richardson, T. L. and Miller, J. J. (1984). Ephaptic interactions contribute to paired pulse and frequency potentiation of hippocampal field potentials. *Exp. Brain. Res.* **54**, 567-570.

Watanabe, S., Hoffman, D. A., Migliore, M. and Johnston, D. (2002). Dendritic K^+ channels contribute to spike-timing dependent long-term potentiation in hippocampal pyramidal neurons. *Proc. Natl. Acad. Sci. USA* **99**, 8366-8371.

Yuste, R. and Tank, D. W. (1996). Dendritic integration in mammalian neurons, a century after Cajal. *Neuron* **16**, 701-716.

Zipser, B. and Bennett, M. V. L. (1976). Responses of cells of the posterior lateral line lobe to activation of electroreceptors in a mormyrid fish. *J. Neurophysiol.* **39**, 693-712.